Atomic displacements effects on the electronic properties of $Bi_2Sr_2Ca_2Cu_3O_{10}$

J.A. Camargo-Martínez
Grupo de Investigación en Ciencias Básicas, Aplicación e Innovación - CIBAIN,
Fundación Universitaria Internacional del Trópico Americano - Unitrópico, Yopal - Colombia,
e-mail: jcamargo@unitropico.edu.co

D. Espitia and R. Baquero
Departamento de Física, CINVESTAV-IPN,
Av. IPN 2508, 07360 México.

Received 26 May 2014; accepted 30 January 2015

The displacements effects of the oxygen atom associated to the Sr-plane (O3) in the electronic properties of $Bi_2Sr_2Ca_2Cu_3O_{10}$ (Bi-2223), have been investigated using density functional theory. We determined intervals of the O3 atomic positions for which the band structure calculations show that the Bi-O bands, around the high symmetry point $\overline{\mathrm{M}}$ in the irreducible Brillouin zone, emerge towards higher energies avoiding its contribution at Fermi level, as experimentally has been reported. This procedure does not introduce foreign doping elements into the calculation. Our calculations present a good agreement with the angle-resolved photoemission spectroscopy (ARPES) and nuclear magnetic resonance (NMR) experiments. The two options found differ in character (metallic or nonmetallic) of the Bi-O plane. There are not any experiments, to the best of our knowledge, which determine this character for Bi-2223.

Keywords: Bi-2223; electronic structure; band structure; Fermi surface.

PACS: 74.72.-h; 71.20.-b; 71.18.+y; 73.20.At

1. Introduction

The $Bi_2Sr_2Ca_2Cu_3O_{10}$ compound (Bi-2223) is a high-temperature superconductor (HTSC) which shows a transition to the superconducting state at $\sim 110K$ [1,2]. There are very few theoretical studies for this compound in the literature in spite of the fact that it is one of the most suitable HTSC materials for applications [3–5]. Also, experimental reports show that the composite CdS/Bi-2223 and the Bi-2212/Bi-2223 intergrowth single crystals display the reentrant superconducting behavior [6,7], which is not yet fully understood.

In a previous work [8] we calculated the electronic properties of Bi-2223 that show the Bi-O pockets problem, which means the presence of Bi-O bands at the Fermi energy (E_F) around the high symmetry point $\overline{\mathrm{M}}$ in the irreducible Brillouin zone (IBZ). This problem appears in all the bismuth cuprates, a result which does not correspond to the experiment. This is an issue that has been present in the literature since long ago [8–15]. H. Lin *et al*. showed that this issue can be solved by doping the bismuth cuprates with Pb [16, 17]. Also, V. Bellini et al., simulated a Bi-O plane terminated (001) surface in $Bi_2Sr_2Ca_1Cu_2O_8$ (Bi-2212) and obtained that the Bi-O pockets become less distinguishable [18].

As it is known, atomic displacements in the crystalline structure generate considerable changes in the electronic properties. Herman *et al*. reported band structures for Bi-2212 that were calculated by displacing the Bi and O atoms, and found significant shifts in the bands [19]. However, their band structures differ greatly from those obtained by other researchers [11].

Based on this idea, in this paper we study the effect of different atomic displacements in the electronic properties of Bi-2223, and found that the displacements of the oxygen atoms associated to the Sr plane induces important changes in the band structure around the $\overline{\mathrm{M}}$ point, displacing Bi-O bands towards higher energies, and avoiding the presence of the Bi-O pockets in the Fermi surface. This simple procedure produces a good agreement between theory and experiment of the electronic properties of Bi-2223.

2. Method of Calculation

In this paper the calculations were done using the full-potential linearized augmented plane wave method plus local orbital (FLAPW+lo) [20] within the local density approximation (LDA), using the wien2k code [21]. The core states are treated fully relativistically, while for the valence states the scalar relativistic approximation is used. We used a plane-wave cutoff at $R_{\mathrm{mt}}K_{\max} = 7.0$ and for the wave function expansion inside the atomic spheres, a maximum value for the angular momentum of $l_{\max} = 12$ with $G_{\max} = 25$. We choose a $17 \times 17 \times 17$ k-space grid which contains 405 points within the IBZ. The muffin-tin sphere radii R_{mt} (in atomic units) are chosen to be 2.3 for Bi, 2.0 for Sr, 1.9 for both Ca and Cu, and 1.5 for O (1.02 for the structure II see below).

3. Structures

In this work, we start from the Bi-2223 compound in a body center tetragonal structure (bct) and space group I4/mmm (D_{4h}^{17}). The structure consists of three Cu-O planes, one Cu1-O1 plane between two Cu2-O2 planes, with Ca atoms between them. Each Cu2-O2 plane is followed by a Sr-O3 and

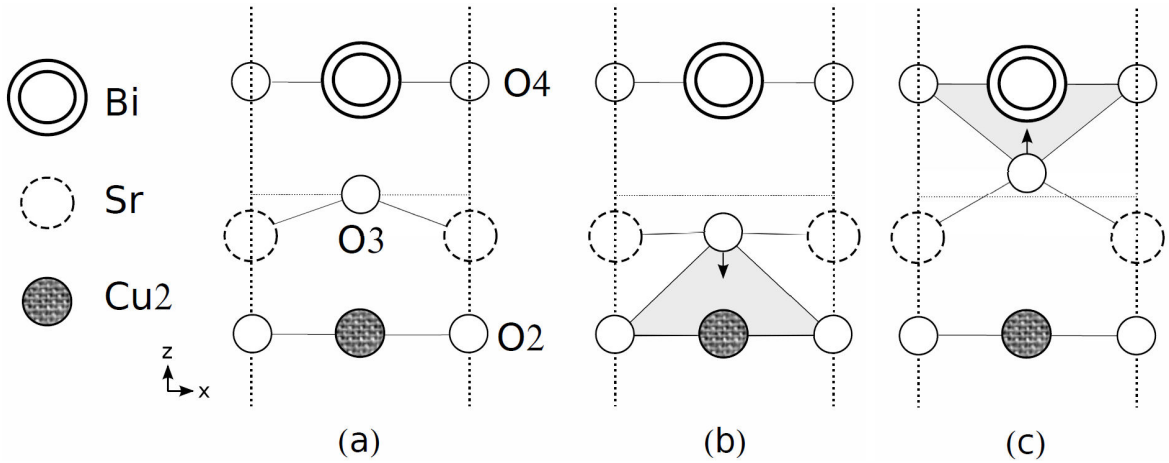

FIGURE 1. Schematic structures for the different atomic configurations a) structure Opt, b) structure I and c) structure II.

TABLE I. The O3 atomic positions and the interatomic distances between Cu2 and O3 ($d_{\text{Cu2-O3}}$) and between Bi and O3 ($d_{\text{Bi-O3}}$) for the different configurations. The intervals for the structures I and II. The data for structure Opt were taken from Ref. 8. The experimental data were taken from Ref. 23.

Structure	O3 site	Interatomic distance (Å)	
	z/c	$d_{\text{Cu2-O3}}$	$d_{\text{Bi-O3}}$
Experiment	0.1454	1.7719	2.4281
Structure Opt	0.1519	2.4946	2.0287
Structure I	0.1335	1.8196	2.7037
Structure II	0.1592	2.7624	1.7609
Structure I Interval (z/c) (0.133-0.134)			
Structure II Interval (z/c) (0.1583-0.16)			

Bi-O4 planes respectively. In a previous work [8] we optimized the c/a ratio and relaxed the internal parameters of the structure taking as A starting point the experimental internal parameters given in Ref 23. Henceforth, we will refer to this optimized structure as structure Opt (see Fig. 1(a)). In the band structure calculations for the structure Opt, the Bi-O pockets appear [8].

R. Kouba *et al.* found that one has to start from the theoretical equilibrium volume *i.e.* to optimize the structure, because the use of the experimental lattice parameters represent an inconsistency [22]. We have checked that starting from the experimental lattice and internal parameters the Bi-O pockets do not appear at E_F at the cost of avoiding the optimization procedure, which as we just mentioned leads to a non-optimal description of the electronic properties.

Taking the optimized internal parameters of the structure as the starting point, we performed small displacements of the positions of the Bi, O4, O3 and Sr atoms in different configurations and found that some of them generate changes in the band structures that remove the Bi-O pockets. The simplest way is just to displace the O3 atoms in two small intervals around the optimized position (see Table I). These intervals are defined in two structures which we labeled as structure I and structure II. It is important to note that O3 atomic positions out of these intervals show the Bi-O pockets back. We will discuss here the resulting electronic properties in two cases when the O3 atoms are displaced by $\sim$0.68 Å towards the Cu2-O2 planes (structure I) and when they are displaced by $\sim$0.27 Å towards the Bi-O4 planes (structure II). See Fig. 1(b) and Fig. 1(c).

In Table I we present the O3 atomic positions and the interatomic distances between Cu2 and O3 ($d_{\text{Cu2-O3}}$), and between Bi and O3 ($d_{\text{Bi-O3}}$) for the different configurations, and the intervals for the structures I and II. The atomic positions of the other atoms in the crystal structure of Bi-2223 remain without changes and can be found in the Ref. [8].

As it can be seen from Table I, the displacements of O3 in the structures I and II produce important changes in the interatomic distances $d_{\text{Cu2-O3}}$ and $d_{\text{Bi-O3}}$. In the structure I the $d_{\text{Cu2-O3}}$ is very close to the the experimental value (the difference is ~ 0.05 Å), while in structure II the $d_{\text{Bi-O3}}$ is ~ 0.67 Å less than the experimental value. As we will see later these features will have consequences in the metallic or nonmetallic character of the Bi-O planes.

4. Results and discussion

4.1. Band structure

In this section we will present the band structures of the different crystalline configurations described in the previous section. The band structure of the structure Opt is shown in Fig. 2. (Notice that $\overline{\text{M}}$ is the midpoint between the Γ and Z along the Σ direction). A detailed analysis of this band structure can be found in the Ref. 8.

In the band structure of the structure Opt we note the presence of five bands crossing at E_F around the $\overline{\text{M}}$ point and in the Z-X direction. These bands are derived from Cu1 d, Cu2 d, and Bi p states. In the Z-X direction (see Fig. 2(b)) there are three bands labeled as α, β, and γ, de-

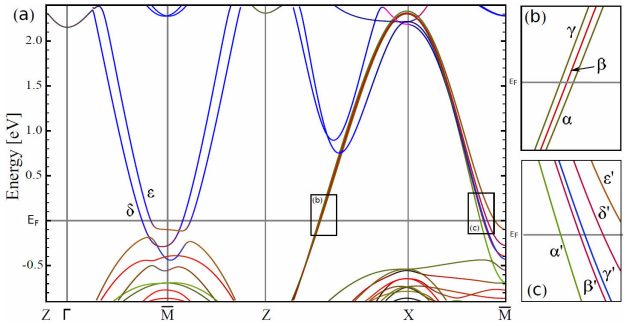

FIGURE 2. (Color online) The band structure of the $Bi_2Sr_2Ca_2Cu_3O_{10}$ compound of the structure Opt. The rectangles in the figure (a) are amplified in Figures (b) and (c) respectively. The blue, red and green lines represent the Bi p, Cu2 d, and Cu1 d respectively. The hybridized states from these bands are represented by their respective color mixture and the black line represents the other states.

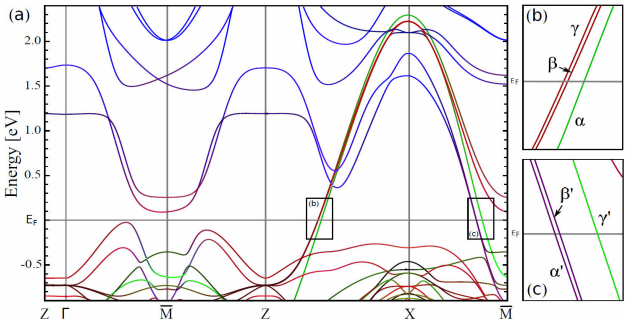

FIGURE 3. (Color online) The band structure of the $Bi_2Sr_2Ca_2Cu_3O_{10}$ compound of the structure I. The rectangles in the figure (a) are zoomed in Figures (b) and (c) respectively. The blue, red and green lines represent the Bi p, Cu2 d, and Cu1 d respectively. The hybridized states from these bands are represented by their respective color mixture and the black line represents the other states.

rived from the Cu-O planes, crossing at E_F (which is characteristic of the HTSC cuprates). The relevant feature here is the presence of Bi-O bands labeled as δ and ε which drop below E_F (~ 0.29 eV) around the $\overline{\text{M}}$ point, hybridizing with the Cu-O bands. This behavior has never been observed experimentally [12–15]. The band dispersion in the Γ-Z direction (perpendicular to the basal plane) is minimal, which means that the bands are strongly two dimensional.

The band structure of the structure I is shown in Fig. 3. We observed that the general behavior of this band structure is similar to the one calculated for the structure Opt, although several important differences are present. It is observed in the band structure that only three bands cross at E_F in two regions, in the Z-X direction and around the $\overline{\text{M}}$ point. In Table II we present in detail the contribution at E_F from the different atomic states.

In the first region (see Fig. 3(b)) there are three bands. Two of these bands are nearly degenerate (labeled as β and γ); these are composed of Cu2 d, O2 p, and O3 p states. The other band (labeled as α) is composed of Cu1 d and, O1 p (see Table III).

In the second region, in the X-$\overline{\text{M}}$ direction (see Fig. 3(c)) there are three bands crossing the E_F. Two of these bands are nearly degenerate (labeled as α' and β'), these are composed of Bi p, O4 p, O3 p, Cu2 d, and O2 p states (see Table II). Here the metallic character of the Bi-O bands is evident. The other band (labeled as γ') is composed of Cu1 d, O1 p, and Bi p states.

The main difference between the structure I and the structure Opt, is present around the $\overline{\text{M}}$ point in the Γ-Z direction (see Fig. 3(a)), where it is observed that the bands derived from hybrids Bi-O and Cu-O states raise above E_F ~ 90 meV, while the bands below E_F (with the same composition that the ones calculated in the structure Opt) reach ~ -25 meV.

It is observed in the band structure of the structure I that some Bi-O bands do not follow a rigid displacement to the energies above E_F. Below E_F important changes are observed in the dispersion of Cu-O bands with presence of Bi-O states around $\overline{\text{M}}$.

The band structure of the structure II is shown in Fig. 4. Just as in the previous case the band structure of the structure II is similar to the one calculated for the structure Opt. Again it is observed in the band structure that three bands cross E_F in two regions, in the Z-X direction and around the $\overline{\text{M}}$ point. In Table III we present in detail the contribution at E_F from the different atomic states.

TABLE II. Detailed contribution (structure I) from the different atomic states to the bands at E_F.

		Bi		O4	O3		Cu1	O1		Cu2	O2	
Direction	Band	$p_{x,y}$	p_z	$p_{x,y}$	$p_{x,y}$	p_z	$d_{x^2-y^2}$	p_x	p_y	$d_{x^2-y^2}$	p_x	p_y
	α	-	-	-	-	-	48%	16%	36%	-	-	-
Z-X	β	-	-	-	11%	-	-	-	-	33%	20%	36%
	γ	-	-	-	11%	-	-	-	-	33%	20%	36%
	α'	7%	65%	8%	4%	4%	-	-	-	5%	-	7%
X-$\overline{\text{M}}$	β'	18%	8%	21%	10%	10%	-	-	-	15%	-	18%
	γ'	-	10%	-	-	-	60%	-	30%	-	-	-

TABLE III. Detailed contribution (structure II) from the different atomic states to the bands at E_F.

Direction	Band	Cu1			O1		
		$d_{x^2-y^2}$	p_x	p_y	$d_{x^2-y^2}$	p_x	p_y
Z-X	α	15%	8%	11%	44%	8%	14%
	β	-	-	-	69%	11%	20%
	γ	40%	10%	22%	19%	-	9%
X-$\overline{\text{M}}$	α'	36%	-	16%	82%	-	18%
	β'	-	-	-	15%	-	18%
	γ'	32%	-	15%	42%	-	12%

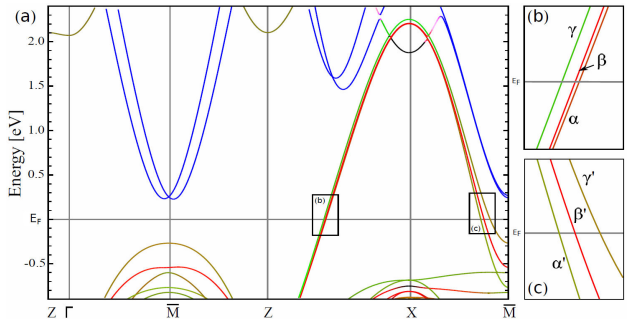

FIGURE 4. (Color online) The band structure of the $Bi_2Sr_2Ca_2Cu_3O_{10}$ compound of the structure II. The rectangles in the figure (a) are amplified in Figures (b) and (c) respectively. The blue, red and green lines represent the Bi p, Cu2 d, and Cu1 d respectively. The hybridized states from these bands are represented by their respective color mixture and the black line represents the other states.

In the first region (see Fig. 4(b)) there are three bands. Two of these bands (labeled as α and γ), are composed of Cu1 d, O1 p, Cu2 d and, O2 p states. The other band (labeled as β) is composed of Cu2 d and O2 p states (see Table III). Note that the α and β bands are nearly degenerate.

In the second region, in the X-$\overline{\text{M}}$ direction (see Fig. 4(c)) there are three bands crossing the E_F. Two of these bands (labeled as α' and γ') are composed of Cu1 d, O1 p, Cu2 d, and O2 p states. The other band (labeled as β') is composed of Cu2 d and O2 p states.

Again around the $\overline{\text{M}}$ point in the Γ-Z direction (see Fig. 4(a)), it is observed that the bands derived from Bi-O states do not cross E_F and are displaced above E_F $\sim$ 230 meV. Notice that in this case (structure II), the Bi-O bands does not contribute to E_F, therefore in this structure, the Bi-O plane is nonmetallic. Now, below E_F the bands derived from Cu-O states reach ~ -270 meV.

Comparing the band structures from structure II with the ones obtained from structure Opt, it is observed a rigid displacement of ~ 0.6 eV of the Bi-O bands toward higher energies. As a result of this, all states associated to the bismuth atoms are now above E_F. Also, the general behavior from the Cu-O bands below E_F show no significant changes.

It is important to note that in the three band structures Fig. 2, Fig. 3 and Fig. 4, the bands mainly derived from the Cu-O planes, which cross the E_F in the Z-X-$\overline{\text{M}}$ directions, show no important differences in its dispersion, although some changes in its composition can be found (see Table II and Table III). These three band structures present strongly two dimensional characters.

4.2. Fermi surface

In Fig. 5 we show the Fermi Surface (FS) of the Bi-2223 compound in an extended zone scheme for the three analyzed structures. A detailed study of the FS for structure Opt is presented in Ref. 8. In this surface the important feature is the presence of the Bi-O pockets around the $\overline{\text{M}}$ point, which are in disagreement with the experimental data [12–15].

It is observed from Fig. 5(b) and Fig. 5(c) that the topology of the FS's is strongly affected by the atomic displacement of the O3. There are three not quite degenerate hole surfaces around the X point, labeled α, β, and γ. These surfaces are derived from Cu-O planes, although the structure I has a contribution of the O3 atoms (see Table II). In these surfaces the most relevant feature is the complete absence of the Bi-O pockets around the $\overline{\text{M}}$ point, in agreement with the experimental results [12–15].

In Fig. 5(b) around the Γ point, spiky sheets appear in the γ surface that are different from the one around the Z point, causing a lower two dimensional character as compared to structure II. Also in structure I, in the X-$\overline{\text{M}}$ direction there is a presence of Bi-O states, contributing to the FS, which was observed in the band structure, as can be seen in Table II.

Mori *et al*. [24] show that the number of bands crossing at E_F (in the nodal direction) is proportional to the number of the Cu-O planes in the multilayer cuprates. LDA electronic calculations present the same feature [8]. The band structures from the structures I and II (see Fig. 3(b) and Fig. 4(b)) show again these three bands crossing at E_F. Two of them are nearly degenerate. The three band splitting is not observed in the experiment due to the degeneration of these bands and the resolution limitations inherent to the experimental equipment [8, 13].

The FS of Bi-2223 measured by angle-resolved photoemission spectroscopy (ARPES) is shown in Ref. 13. In that

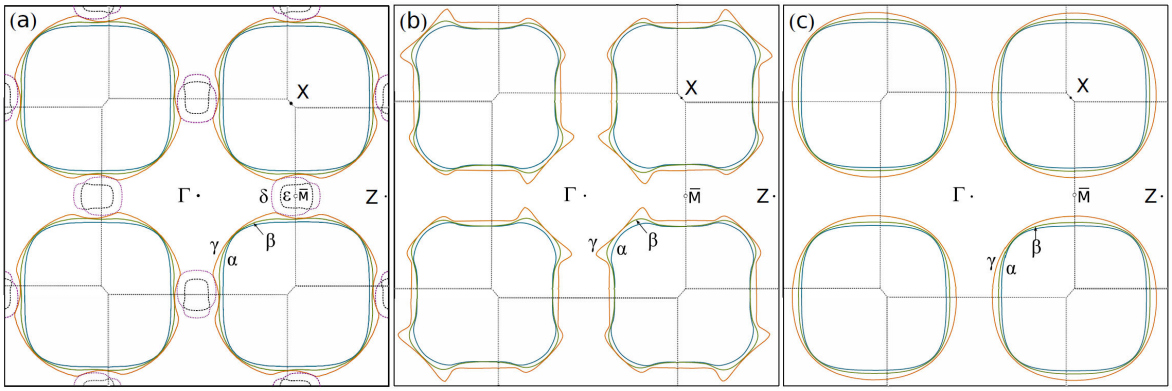

FIGURE 5. (Color online) The Fermi Surface (FS) at $k_z = 0$ of $Bi_2Sr_2Ca_2Cu_3O_{10}$ in an extended zone scheme. (a) shows the FS for structure Opt. The Bi-O pockets are represented by violet and black lines (dashed lines). (b) and (c) show the FS for structure I and II respectively. These two FS's do not show Bi-O pockets.

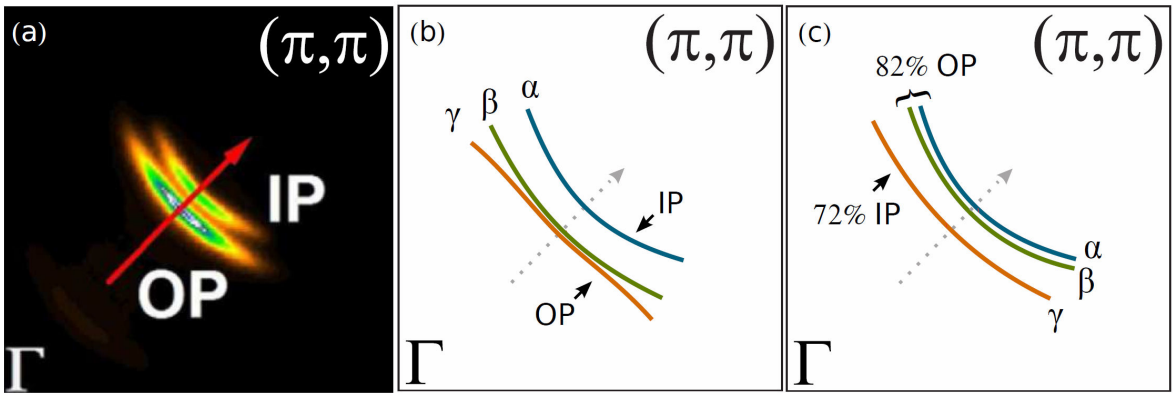

FIGURE 6. (Color online) (a) The Fermi surface (FS) of Bi-2223 measured by ARPES [13] in the nodal direction. (b) and (c) Schematic FS showing the band splitting in the structures I and II respectively.

work they found two surfaces on the nodal direction (see Fig. 6(a)), that were assigned to the outer copper planes Cu2-O2 (OP) and to the inner copper plane Cu1-O1 (IP) and suggest the possibility that the OP's are degenerate. Other experimental work with the same technique does not report this band splitting [14, 15].

In Fig. 6 the comparison between the experimental FS [13] and the calculations done in this work for structures I and II in the nodal direction are shown. A good agreement with the experiment can be observed here.

In the FS of structure I (Fig. 6(b)) it is observed that the β and γ surfaces are nearly degenerate and derived from the Cu2-O2 planes (OP) with a contribution of the O3 $p_{x,y}$ states (see Table II), while the α surface is derived from the Cu1-O1 plane (IP). This result shows a good agreement with the composition of the surfaces assigned by Ideta et. al. in the experiment reported in Ref. 13.

In the FS of structure II (Fig. 6(c)) it is observed that the α and γ surfaces are derived from the hybridization of the Cu2-O2 and Cu1-O1 planes (OP+IP), while the β surfaces ARE derived from the Cu2-O2 planes (OP). In this case the α and β surfaces are nearly degenerate, which are mainly derived from Cu2-O2 planes (82% OP), while the γ surface is mainly derived from Cu1-O1 plane (72% IP). The composition that we got from our calculations slightly differs from the ones assigned by Ideta *et al*.

Notice that structure I agrees with the experimental assignment of the OP's as being degenerate(Fig. 6(b)). Structure II (Fig. 6(c)) indicates that it is the OP degenerate surfaces, in disagreement with the assignment of Ideta *et al*. [13].

On the other hand, nuclear magnetic resonance (NMR) studies of the Bi-2223 compound show that the hole concentration of the OP is larger than that of the IP [25,26], in agreement with our calculations in both cases.

4.3. Density of states and total energy

The Fig. 7 shows both the total Density of States (DOS) and the atom-projected density of states (pDOS) for the structures Opt, I, and II. The analysis for the DOS of the structure Opt is presented in the Ref. 8.

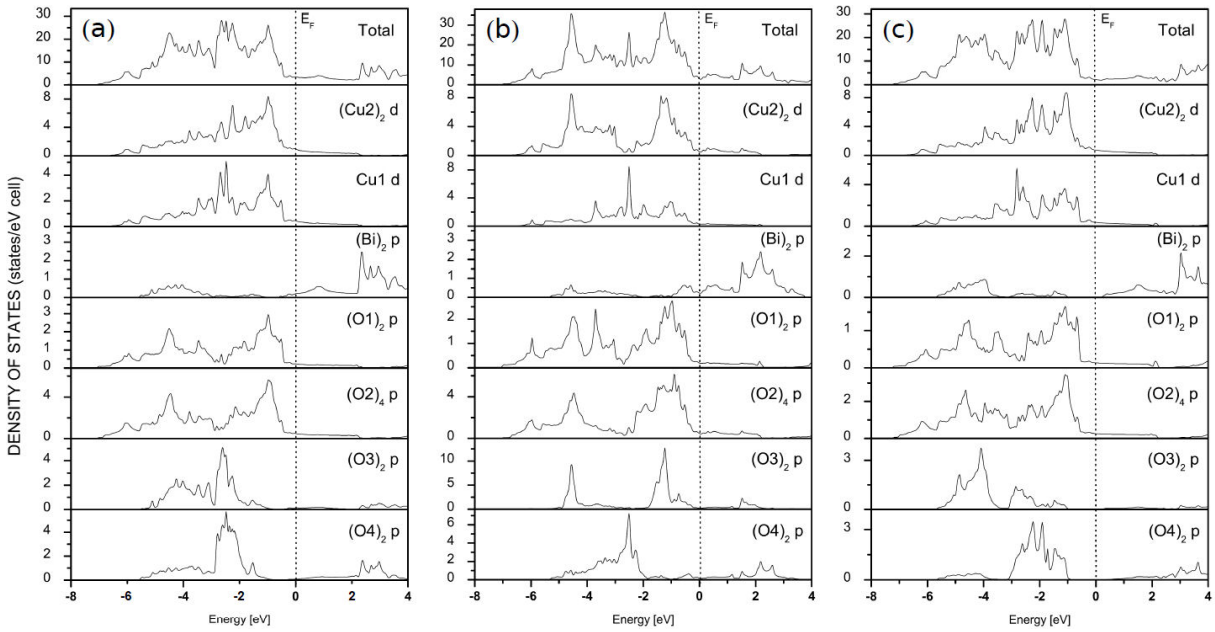

FIGURE 7. Total and atom-projected density of states for $Bi_2Sr_2Ca_2Cu_3O_{10}$ for the structure Opt (a), structure I (b) and, structure II (c). Note the change of scale for each atom contribution.

TABLE IV. Atomic contributions to the density of states at the E_F, N(E_F), total N(E_F) and total energy for structures Opt, I, and II. The values are given in units of states/eV-atom, states/eV-cell and Ry respectively. The data for structure Opt were taken from Ref. 8.

	Atomic state							Total	Total energy
Compound	Cu2 d	Cu1 d	Bi p	O1 p	O2 p	O3 p	O4 p	N(E_F)	(Ry)
Structure Opt	0.47	0.44	0.10	0.12	0.12	0.06	0.04	3.55	-113112.127
Structure I	0.27	0.34	0.12	0.10	0.12	0.07	0.09	3.14	-113111.839
Structure II	0.37	0.38	-	0.07	0.06	-	-	2.15	-113108.197

As we just saw the displacement of the O3 atomic position in the crystalline structure generates significant changes in the band structure and in the FS. As expected, these changes are also visible in the DOS. Comparing the DOS of the structure Opt with the structure II we found that the general behavior is similar (as observed in the band structure and the FS). On the contrary, important changes are observed in the DOS in the structure I.

The most important feature in the DOS for the structure II is the absence of any contribution of the Bi p, O3 p, and O4 p states at E_F, a fact that leads to a lower density of states at E_F, N(E_F), which is 2.15 states/(eV-cell) as compared to 3.55 states/(eV-cell) in structure Opt and 3.14 states/(eV-cell) in structure I. In Table IV we presented both the atomic and the total contributions to the N(E_F) for structures Opt, I, and II.

In the DOS of the structure I (see Fig. 7(b)) it is observed that the Bi-O planes have a contribution at E_F, and as a consequence the Bi-O planes have a metallic character (see Table IV). In the DOS of structure II a shift with respect to the structure Opt of the DOSp from Bi p and O4 p states towards higher energies from the E_F is observed (see Fig. 7(c)). This results in a nonmetallic character of the Bi-O planes (see Table IV).

An explanation for the metallic or nonmetallic character of the Bi-O planes can be understood as follows. The ionic character of the Bi atoms in the crystalline structure tends to attract electrons into the Bi-O planes competing with the affinity for the electrons towards the Cu-O planes [16]. This may involve the charge transfer between the Cu2-O2 and Bi-O4 planes. This charge transfer is possible by the interaction of the O3 atoms with the aforementioned planes. In the structure I, when O3 is closer to the Cu2-O2 planes it acts like a bridge for the charge transfer to the Bi-O4 planes, giving these planes the metallic character observed in one of our calculations. This explains the possible reason why the structure I has a larger contribution of Bi-O states at E_F than the structure Opt (see Table IV). On the other hand in the structure II, O3 is closer to the Bi-O4 planes (away from the Cu2-O2 plane) which nullify the charge transfer between these planes, explaining the nonmetallic character of the Bi-O planes.

We found two configurations that remove the pockets around the $\overline{\text{M}}$ point associated to the Bi-O planes. The relevant difference between these configurations lies in the metal-

lic (structure I) or nonmetallic (structure II) character of the aforementioned planes.

Experimental results using scanning tunneling microscopy (STM), show that the Bi-O planes are nonmetallic in Bi-2212 [27–30]. To the best of our knowledge there are not any experiments that define the metallic or nonmetallic character of the Bi-O planes in Bi-2223, except for the report presented by K. Asokan *et al*. using X-ray absorption near edge structure (XANES), that shows a metallic character of the Bi-O planes for Bi-2223 and Bi-2212 [31], the last one is in disagreement with the previous works just mentioned. However, the nature of the Bi-O planes character for Bi-2223 needs to be tested with more experiments. The lack of enough experimental data for Bi-2223 does not allow us to choose which of the two studied configurations completely agrees with the experiments. Knowing the Bi-O planes character would permit us to support (or not) the assignation done by Ideta *et al*. in the FS compositions in the nodal direction [13]. If the metallic case (structure I) is supported by the experimental results, it would confirm that the surfaces derived from OP's are closer to the Γ point which would agree with Ideta *et al*., while if the nonmetallic case happens, our calculations suggest that the surface that is closer to the Γ point derives mainly from states associated to IP.

In Table IV is observed the total energy calculated in the system with structures Opt, I y II. The systems with structures I and II present total energies higher than the structure Opt, *i.e*. those O3 atomic displacements do not lead the system to a minimal energy state. Thus, the O3 positions proposed which remove the Bi-O pockets does not represent a minimal local of the total energy system. This point requires a more detailed analysis.

Finally, we also calculated the total spin magnetic moment per cell for the structures Opt, I, and II and obtained $\sim$0.01 μ_B, $\sim$0.02 μ_B, and $\sim$0.03 μ_B respectively. This implies that the compound does not exhibit a significant magnetic character at T=0 K.

5. Conclusions

In this paper we addressed the so called Bi-O pockets problem, namely, the appearance of states at the Fermi energy that are attributed to the Bi-O plane in theoretical ab initio calculations of the electronic band structure of Bi-cuprates, and that are in contradiction with experiment. These pockets disappear in two ways, either by using the experimental parameters and avoiding any optimization procedure (as we have checked) or by doping with 25% of Pb [16]. R. Kouba *et al*. [22] points to the need of the optimization procedure to get an electronic band structure that reproduces properly the electronic properties of the system in consideration.

So, we have considered several ways in which the presence of Bi-O pockets in the Fermi surface can be avoided without doping and keeping the optimization procedure previous to the ab initio calculation, in agreement with the experiment. We perstructureed small displacements of the positions of the Bi, O4, O3 and Sr atoms in several configurations and found that some of them generate changes in the band structures that remove the Bi-O pockets that appear around the high-symmetry point $\overline{\mathrm{M}}$. These pockets appear in all the theoretical ab initio electronic calculations of bismuth cuprates. The simplest way to remove the Bi-O pockets that we found is to displace the O3 atoms (the ones associated to the Sr-O planes) within two small intervals around its optimized position. Positions out of these small intervals lead to calculations that again show the Bi-O pockets. We studied the effect of an atomic displacement of the O3 atoms in two configurations which we called structure I and structure II in the electronic properties of $Bi_2Sr_2Ca_2Cu_3O_{10}$ using the LDA. In both cases the Bi-O pockets are removed. The relevant difference between these two configurations lies in the metallic (structure I) or nonmetallic (structure II) character of the Bi-O planes. This procedure is absent of any doping. Our calculations for both structures present a good agreement with the experimental results measured by angle-resolved photoemission spectroscopy (ARPES) and nuclear magnetic resonance (NMR). Since the experimental situation of the character (metallic or nonmetallic) of the Bi-O planes in Bi-2223 has not been totally clarified, we cannot decide which of the two structures reproduces more exactly the experimental results. Both, we emphasize, the Bi-O pockets are not observed in the Fermi surface.

6. Acknowledgments

The authors acknowledge to the GENERAL COORDINATION OF INFORMATION AND COMMUNICATIONS TECHNOLOGIES (CGSTIC) at CINVESTAV for providing HPC resources on the Hybrid Cluster Supercomputer Xiuhcoatl and to the Instituto de Ciencia y Tecnología del Distrito Federal under the contract ICyTDF/268/2011, that have contributed to the research results reported within this paper. D.E. acknowledges the hospitality of the Department of Physics at Cinvestav.

1. J. L. Tallon *et al*., *Nature* **333** (1988) 153.
2. J. M. Tarascon *et al*., *Phys. Rev. B* **38** (1988) 8885.
3. H. Kitaguchi and H. Kumakura *MRS Bulletin: Advances in Bi-Based High-Tc Superconducting Tapes and Wires* **26** (2001) 121.
4. T.J. Arndt, A. Aubele, H. Krauth, M. Munz, B. Sailer, and A. Szulczyk, *IEEE Transactions on Applied Superconductivity* **13** (2003) 3030.
5. W. Hassenzahl *et al*., *Electric power applications of supercon-*

ductivity. Proceedings of the IEEE. Special Issue on Applications of Superconductivity **92** (2004) 1655.

6. E. Díaz-Valdés, G.S. Contreras-Puente, N. Campos-Rivera, C. Falcony-Guajardo and R. Baquero, *arXiv:1101.0277* [cond-mat.supr-con].
7. Y. Zhao *et al*., *Phys. Rev. B* **51** (1995) 3134.
8. J. A. Camargo-Martínez, Diego Espitia and R. Baquero, *Rev. Mex. Fis.* **60** (2014) 39.
9. S. Massidda, J. Yu and A. J. Freeman, *Phys. C* **152** (1988) 251.
10. H. Krakauer and W.E. Pickett, *Phys. Rev. Lett.* **60** (1988) 1665.
11. D.J. Singh and W.E. Pickett, *Phys. Rev. B* **51** (1995) 3128.
12. A. Damascelli *et al*., *Rev. Mod. Phys.* **75** (2003) 473.
13. S. Ideta *et al*., *Phys. Rev. Lett.* **104** (2010) 227001.
14. H. Matsui *et al*., *Phys. Rev. B* **67** (2003) 060501.
15. D.L. Feng *et al*., *Phys. Rev. Lett.* **88** (2002) 107001.
16. Hsin Lin *et al*., *Phys. Rev. Lett.* **96** (2006) 097001.
17. H. Lin, *Topics in electronic structure and spectroscopy of cuprates* (2008). Physics Dissertations. Paper 14. http://hdl.handle.net/ 2047/d10016363
18. V. Bellini *et al*., *Phys. Rev. Lett.* **69** (2004) 184508.
19. F. Herman *et al*., *Phys. Rev. B* **38** (1988) 204.
20. O.K. Andersen, *Phys.Rev.B* **12** (1975) 3060.
21. P. Blaha, K. Schwars, G.K.H. Madsen, D. Kvasnicka, and J. Luitz, *WIEN2K:Full Potential-Linearized Augmented Plane waves and Local Orbital Programs for Calculating Crystal Properties*, edited by K. Schwars, Vienna University of Technology, Austria, (2001).
22. R. Kouba, C. Ambrosch-Draxl, and B. Zangger, *Phys. Rev. B* **60** (1999) 9321.
23. X. Zhu, S. Feng. J. Zhang, G. Lu, K. Chen, K. Wu, and Z. Gan, *Modern Phys. Lett. B* **3** (1989) 707.
24. M. Mori, T. Tohyama, and S. Maekawa, *Phys. Rev. B* **66** (2002) 064502.
25. A. Trokiner *et al*., *Phys. Rev. B* **44** (1991) 2426.
26. H. Kotegawa *et al*., *J. Phys. Chem. Solids* **62** (2001) 171.
27. M. Tanaka *et al*., *Nature* **339** (1989) 691.
28. M. Tanaka *et al*., *J. Vac. Sci. Technol. A* **8** (1990) 475.
29. S.M. Butorin *et al*., *Phys. Rev. B* **51**, 11915 (1995).
30. S. Sugita *et al*., *Phys. Rev. B* **62** (2000) 8715.
31. K. Asokan *et al*., *J. Electron Spectrosc.* **114** (2001) 837.